Holographic interferometry using photorefractive crystals for quantitative phase measurement on large objects

M.P. Georges and Ph.C. Lemaire

Centre Spatial de Liège - Université de Liège

Parc Scientifique du Sart Tilman, Avenue du Pré-Aily

4031 ANGLEUR (LIEGE) - BELGIUM

ABSTRACT

We recently have presented a real-time holographic interferometer using sillenite crystals connected with phase-shifting for quantitative measurement of diffuse objects deformations. In our basic set-up, the crystal, sandwiched between two polarizers, is set in front of the optical head and followed by a CCD camera with an imaging objective. With this system, for conventional objects and using 2.2 Watts of Ar3+ laser power @ 514 nm, interferograms can be observed on object fields of about 30 cm x 20 cm (crystal size 1 cm x 1 cm and 26 mm objective focal length). In this paper we present investigations to increase the observed field in the existing system and to be able to use lower power lasers. Since setting the object at larger distances should lead to an unsufficient luminous level for hologram recording, we have proceeded by different ways. First, we use shorter focal length objectives, giving a larger field-of-view, and larger crystals have to be used in this case to avoid vignetting. Second, we use a large aperture frontal objective in order to collect more light and that images the object on the crystal, the final image being observed through relay imagery.

Keywords : Holographic interferometry, photorefractive crystals

1. INTRODUCTION

Attractive alternative media for hologram recording in holographic interferometry (HI)[1] are the photorefractive crystals (PRCs) of the sillenite family ($Bi_{12}SiO_{20}$ (BSO), $Bi_{12}GeO_{20}$ (BGO), $Bi_{12}TiO_{20}$ (BTO)).[2-9] They can store phase holograms through refractive index modulation. The process is dynamic and reversible. In these crystals, the charge migration responsible of the hologram recording can take place under thermal diffusion (diffusive regime) and under an applied bias electric field (drift regime).

In HI, the superimposition of the waves, corresponding to the two states of the tested object, leads to an intensity pattern that varies in function of the phase difference between both interfering fields. The interferogram has an intensity profile $I(u,v)$ given in each point (u,v) of an observation plane by :

$$I(u,v)= I_0(u,v)[1+ m(u,v) \cos(\phi(u,v))] \quad (1)$$

where $I_0(u,v)$ is the average intensity of the pattern, $m(u,v)$ the modulation of the interference and $\phi(u,v)$ the phase difference between the diffracted and transmitted wavefronts. In order to obtain the quantitative difference in term of displacement or deformation of the object, the quantity $\phi(u,v)$ has to be determined from the intensity pattern (1). The phase-shifting method is currently used to calculate $\phi(u,v)$ but requires at least 3 interferograms that are shifted in phase between each other.

0-8194-2026-3/96/$6.00

Despite the dynamical behaviour of PRCs, we have shown the possibility to use them in real-time HI with diffuse objects in connection with a phase-shifting algorithm.[7,8] In the real-time process, a first hologram is recorded, the object undergoes a deformation and the subsequent interferogram is observed by continuous readout. Due to the low level of light coming from the object, the storage time of the first hologram in our crystal is long enough to permit capture of the required phase-shifted interferograms. The main limitation of this method is that the object must not move between the acquistions.

In our basic set-up (figure 1), the laser beam, provided by an Ar laser emitting up to 2.2 Watts at 514 nm, is separated in object and reference beams by means of a variable beamsplitter (VBS) in order to have the maximum flexibility for the intensity ratio R ($I_{readout}/I_{object}$), which is important for optimizing the signal-to-noise ratio. In the reference arm, the beam is collimated in order to cover the crystal input face, while in the object arm, the beam is let diverging in order to illuminate large objects. Shutters (SH1 and SH2) are placed in both arms to provide the holographic recording-reading sequence. The phase-shifting is introduced by translating a plane mirror in the path of the reference beam by means of a piezoelectric translator (PSPZT). The holographic head consists in the combination of a first dichroic polarizer (P_1), a photorefractive crystal (C), a second polarizer (P_2), followed by a CCD camera with an imaging objective. The crystal orientation (input face $\perp$ <-110>) are chosen such that, if the grating wave vector $\boldsymbol{K}$ resulting from object and reference beams interference is parallel to crystallographic axis <110>, the diffracted beam linear polarization can be set perpendicular to that of the transmitted object beam by adequate orientation of P_1. This feature is only possible when diffusion regime is used with sillenite crystal (anisotropic self-diffraction) as pointed out by different authors.[5,10-12] In real-time HI based on this principle, one can easily adjust the intensity balance between the diffracted and the transmitted wavefronts, by means of the second polarizer P_2, in order to maximize the modulation of the interferogram.

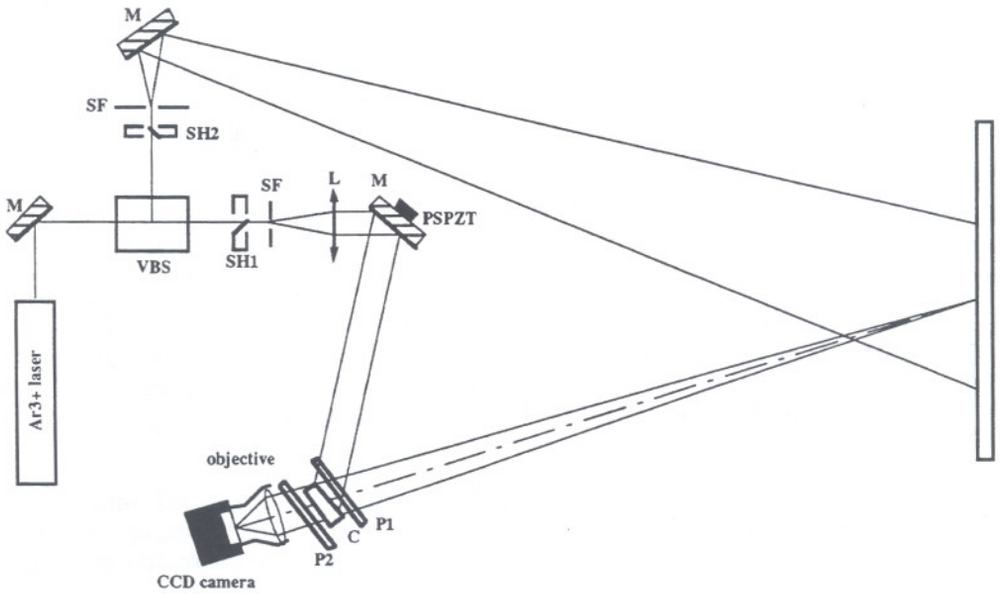

Figure 1. Scheme of the basic holographic interferometer.

The field of view of our system is guided by the sensitivity and the size of the crystal. The first one influences the quantity of light that has to be incident on the crystal for a sufficiently fast recording in regards of the environmental perturbations (vibrations, air turbulences, ...). As the recording time which is inversely proportional to the total incident intensity (sum of the reference and the object intensities), one should use a reference beam as intense as possible to have a fast recording. Nevertheless due to optical surfaces imperfections of the crystal and polarizers, light diffusion

occurs and we have to use a compromise between the diffracted intensity and the perturbative diffusion. So for a given incident light power, the object has to be close enough to the crystal. In our first investigation with a crystal of BSO (from Sumitomo with 1 x 1 cm^2 optical face), we observed that for practical application the object beam intensity at the level of the crystal (after P_1) must be at least about 8 to 10 $\mu Watt/cm^2$. This level is reached, for white diffuse objects set at about 1.2 meter with 2W laser output. We had found an optimum value for $R=I_{ref}/I_{obj}$ of about 30. The second one limits the angular field-of-view of the usable imaging objective because of the vignetting, and as a consequence, its focal length must not be to short. For example, with the BSO described above, we are practically limited to a 26 mm focal length objective. With the maximal object distance of 1.2 m and for a CCD sensor of 6.5x5 mm^2, the observed area is typically 30x20 cm^2.

Our goal is to extend the performances of this first system with the double aim to visualize either 1 m^2 objects with the present Ar laser of 2W, or 0.25 m^2 objects with a power of about 400 mW (corresponding to small portable cw diode pumped frequency doubled YAG laser).

There are different ways to overcome the above described limitations. First, crystals can be grown now with a good optical quality to about 3x3 cm^2 of optical face. Different species of BSO and BGO have been then acquired. Second, a objective lens can be placed in front of the crystal in order to collect light and to image the object at the level of the crystal. The image is then observed by the CCD via a second relay imagery.

2. PRESENTATION OF DIFFERENT OPTICAL SYSTEMS.

Three systems have been investigated for the holographic head (figure 2). All involve a larger crystal of BGO:Cu with an optical face of 28x27 mm^2 and a thickness of 2.6 mm which has been grown by Prof. J. C. Launay at University of Bordeaux (PRAME). The first one, refered as system1 (S1), is the system described above. Both other systems, systems 2 (S2) and 3 (S3) have the same frontal objective lens (O1). The second stage of S2 is simply another lens objective O2, attached to the CCD camera, which images the intermediate image close to the crystal. The second stage of S3 is a 4f-system enabling filtering of the light (in order to possibly reduce high spatial frequency diffusion).

We wish to compare the systems with respect to a given object area to cover. We impose the width of the CCD sensor (6.5 mm) to image a minimum 50 cm object width. We have tried different camera objectives commercialy available. An important condition is that these objectives must have an aperture as large as possible, in order to collect a maximum of light. Focal length of the frontal objective O1 in S2 and S3 must be well correctly chosen in order to have a back focal plane sufficiently far from the objective in order to place the crystal and to illuminate it completely with the reference beam. Note that this can be critical because the angle of maximum efficiency of the crystal appears between 45° and 60° (depending on the species), in the diffusive regime considered here.

Table 1 summarizes the different configurations that will be used. The different listed quantities are the focal length of the different objective lenses (f_{O1}, f_{O2}, f_{O3}), the distance d between the object and either the crystal, or the frontal objective, the intermediate image size formed by the frontal objective close to the crystal and the final image size at the level of the CCD.

An important feature is that, with these parameters, the intensity of object beam at the level of the crystal is 10$\mu W/cm^2$ for S1 with 2 W laser output but also for S2/S3 with only 400 mW laser output. This shows the potentiality of the latters compared to S1 in term of light collection.

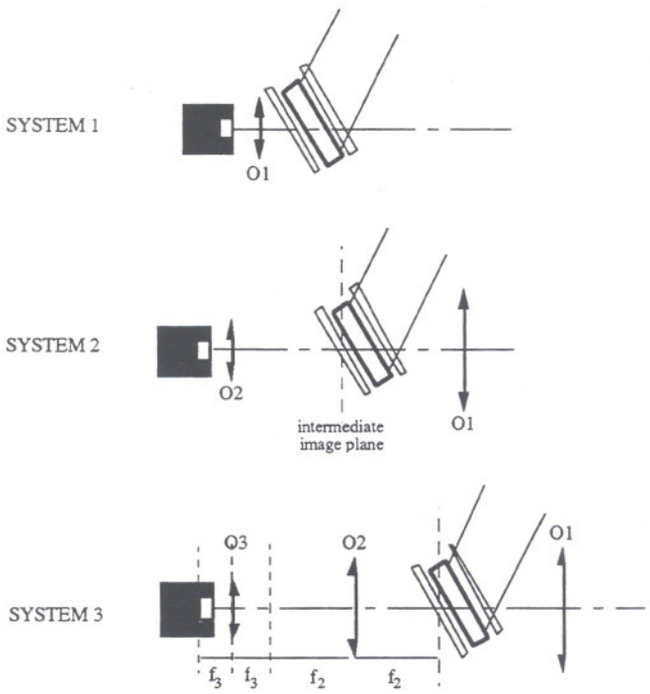

Figure 2. Scheme of the three systems

	System1	System2	System3
f_{O1} (mm)/aperture	16 / 1.4	50 / 1.2	50 / 1.2
f_{O2} (mm)	-	26 / 1.1	80 / 1.9
f_{O3} (mm)	-	-	16 / 1.4
d (m)	1.3	1	1
intermediate image size (mm)	-	26.5	26.5
final image size (mm)	6.5	6.5	5.3

Table 1. Summary of the relevant parameters for the different systems.

3. COMPARATIVE CHARACTERIZATION OF THE SYSTEMS

1°) The recording time

The angular distribution $\Delta\theta$ of the object field entering in one point of the crystal is larger in systems with frontal objective than in the other one. For S2/S3, this distribution is given in function of the aperture and the back focal plane distance, i.e., for the parameters listed above, $\Delta\theta=38°$ in the center of the field-of-view. For S1, it is given by the object size and distance, i.e. $\Delta\theta=11°$.

The diffraction efficiency being dependent on the angle between object and reference writing beams, and since the latter is collimated, this could have the consequence that part of the object rays coming from one point through O1 do not enter in the crystal at the optimum angle, by vertue of what part of the collected light do not participate to the hologram recording.

A good figure of merit for assessing this is to measure, for both S1 and S2/S3, the time needed for the hologram recording because it is inversely proportional to the incident intensities that interfere in the crystal.

We have carried out the experiment consisting of measuring the building up of the hologram using a large diffusive panel as object. We have placed a photodetector instead of the CCD camera and recorded the signal diffracted after all imaging stages for S1 and S2. It is not useful to perform this measurement for S3 since it does not make any difference on the recording characteristics. The object beam intensity is 10 $\mu W/cm^2$ (S1 with 2 W and S2 with 400 mW of incident light power on the object) and the reference intensity varies. The temporal behaviour of the recording is of the type $V=V_0[1-\exp(-t/\tau_{rec})]$ and figure 3 plots the recording time τ_{rec} for different total intensities and for both systems. It appears clearly that both curves match, indicating that the recording occurs in the same manner whatever the system, and that the angular distribution spreading plays no important role on the hologram recording.

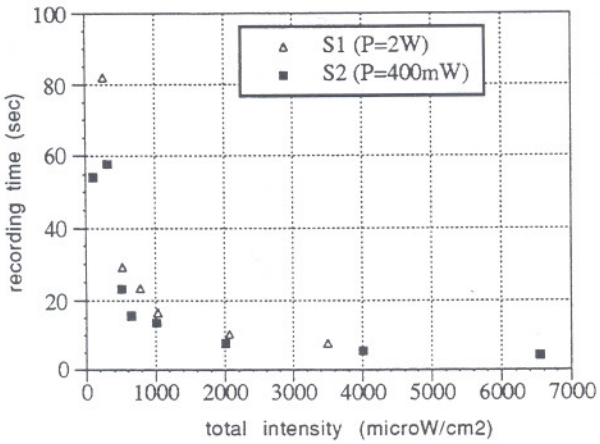

Figure 3.

2°) The modulation of the interferogram observed

After the crystal, one has the superimposition of different wavefields (figure 4) : the transmitted (direct) object beam (in grey), the diffracted beam (in hachured), the light coming from the readout beam and that diffuses by the crystal toward the detector (in white) and, finally, any parasitic diffused light (not shown). Because the input polarizer is not perfectly linear, the transmittance profile is elliptic. The maximum intensities of the transmitted, diffracted and diffused lights are respectively called P_t, P_d and P_n. The diffuse part interfere with other component with very high spatial frequencies in comparison with object interferogram and in consequence is considered as an average intensity . The respective intensities after P_2 are called $I_t(\alpha)$, $I_d(\alpha)$ and $I_n(\alpha)$ and obviously are function of the angle α made by the P_2 polarization axis and P_d.

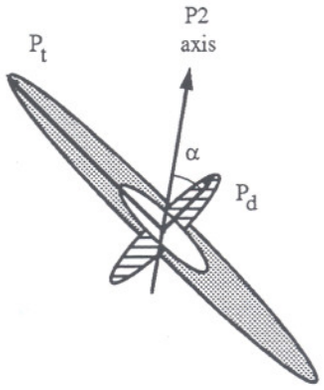

Figure 4.

The modulation m in each point of the interferogram given by (1) is classically defined by:

$$m=\frac{I_{max}-I_{min}}{I_{max}+I_{min}}=\frac{2\sqrt{I_d I_t}}{I_0}=\frac{2\sqrt{I_d I_t}}{I_d+I_t+I_n} \qquad (2)$$

where I_{max} and I_{min} respectively are the maximum and minimum intensities observed in the interferogram. For an inteferometer without noise (I_n=0), the maximal modulation m_{max} that could be reach is 1. This is the case when $I_t(\alpha_{max})=I_d(\alpha_{max})$, thus for a correctly chosen angle. With noise, the modulation at this angle can be written as

$$m_{max}=\frac{1}{K+1} \qquad (3)$$

where

$$K=I_n(\alpha_{max})/2I_t(\alpha_{max}) \qquad (4)$$

In order to compute the maximal modulation that can reach the interferometer for each system, one then has to measure I_d and I_t, calculate the angle α_{max}, measure I_n at α_{max} and finally calculate K.

Measurement of I_d is only possible at α=0° during the readout with P2 aligned along I_d . This has been carried out at 514 nm in the same experiment than the measurement of the recording time. Figure 5 shows $I_d(\alpha=0°)$ for the different systems with the laser output such as the object beam has an intensity of 10 $\mu W/cm^2$.
It is understood that this intensity is not the intrinsic intensity diffracted by the crystal but the part of it that reach the detector after all imagery. From the graph is is clear that the intensity is higher in S1 than in S2 and S3 because the

number of optics is higher, the relative aperture is smaller and the geometrical factor are different. This indicate also that the sensitivity of the CCD camera must be well chosen in function of intensity emerging from the imagery.It is also important to note that it is not necessary to increase to much the readout intensity because in each case, the diffracted intensity do no longer increase.

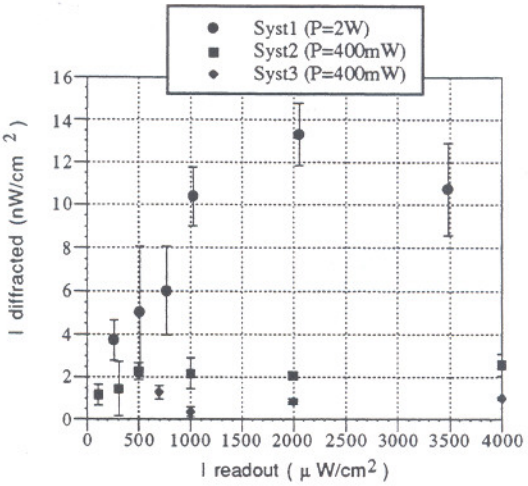

Figure 5.

I_t and I_n have been measured with a photodetector for different orientations of polarizer P2. The object beam intensity is still 10 μW/cm^2 and the readout intensity has been fixed at 3400 μW/cm^2. Figure 6.a, b and c show the results for, respectively, S1, S2 and S3. It is clear that the amount of diffusion is considerably higher for S2/S3 than for S1. This the consequence of the imaging step at a location close from the crystal and the polarizers. Also the levels detected are in good agreement with the results obtained for the diffracted intensity measurements. The profiles look like the Malus law plus, in the case of I_n, an offset coming from parasitic light.

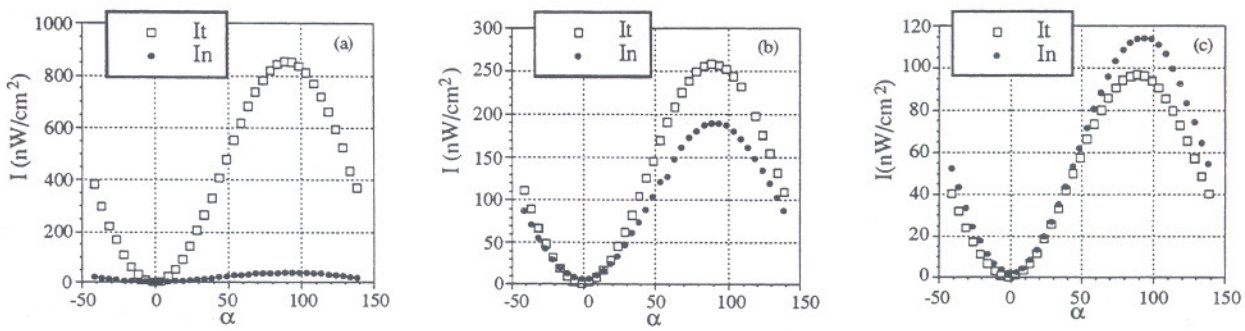

Figure 6.

The angle α_{max} of correct balance between I_d and I_t can be now calculated by considering the following equality

$$I_d(0°)\cos^2(\alpha_{max}) = I_t(90°)\sin^2(\alpha_{max}) \quad (5)$$

Afterwards the curves of I_n and I_t are fitted with a sine squared function and one deduces the factor K by dividing the values of the fitted curves at α_{max} and the maximum modulation can be determined using (3). The results are summarized in table 2

System	α_{max}	m_{max}
1	6.8°	0.89
2	5°	0.5
3	5.7°	0.48

Table 2.

4. RESULTS

We have measured the deformation of a large panel reflecting diffusively. It has a dimension of 60 x 60 cm^2 and is clamped to a metallic mount in order to have sufficient stability. Due to the rectangular shape of our CCD the observed area is 50 x 40 cm^2 . The reference intensity is fixed at 2000 $\mu W/cm^2$. The deformation is given by a static load at the rear side of the panel. The phase-shifting has been used at the readout for computing the phase map of the deformation.

Figure 7 shows the phase map (modulo 2π) of a deformation acquired with S1 and 2W of laser output. The object is placed at 1.3 m of the holographic head. The effective incident power on this one is 1 mW/cm^2. The modulation effectively measured in the corresponding interferograms is typically 0.7. This value is lower than predicted by our preliminary measurement. It is probably due to the fact that some parasitic light, which appears when the output polarizer P2 is set in order to optimize the interferogram contrast, has not been taken into account in that measurement.

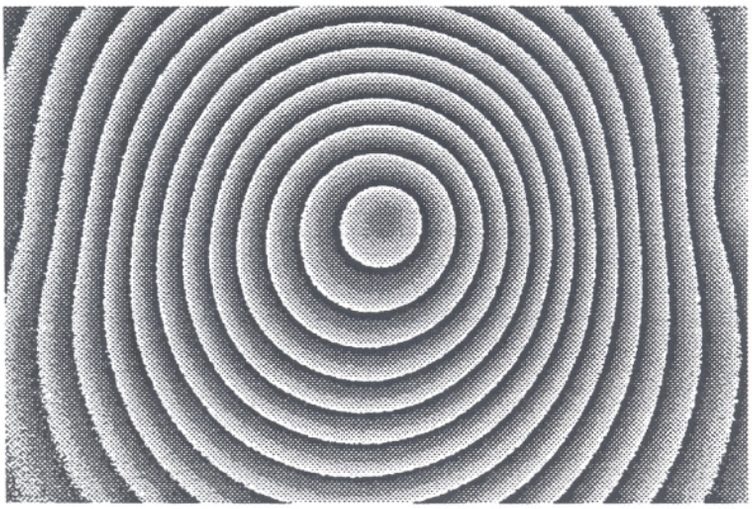

Figure 7.

Figure 8 shows the same kind of deformation acquired with S2 at 400 mW of laser output. The object is placed at 1 m of the holographic head. The effective incident power on this one is 0.4 mW/cm^2 The modulation effectively observed in the corresponding interferograms is in good agreement with preliminary measurements; 0.52 in the center of the field and lower than 0.5 at the edges. This variation is due to the fact that the illumination level at the edges of the object is lower than in the center. This lower modulation, combined with the lower level of diffracted light collected by the system, also explained the noisy border of the final phase image. This example shows clearly that the objective of a field of view of 1 m2 with this system is realizable with 2 W of laser output power and the object placed at a larger distance (≈ 2m)

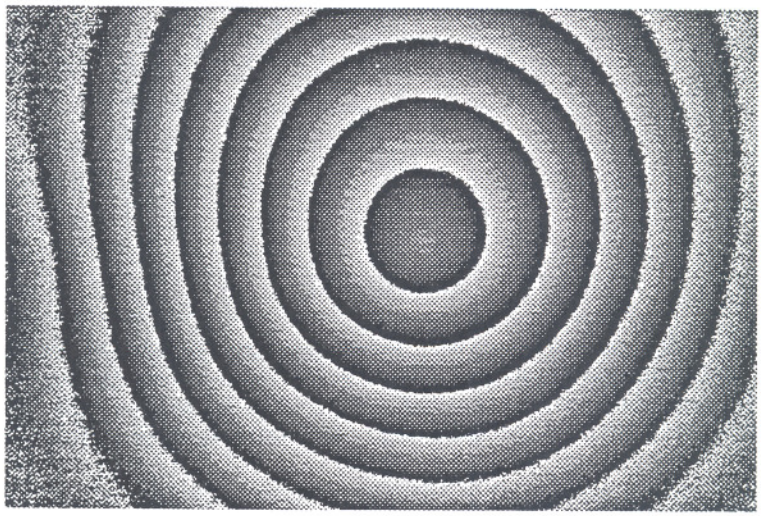

Figure 8.

5. CONCLUSION

System 1 without frontal objective can observe object area of typically 50x50 cm2 (depending on the CCD size and shape), using 2W of laser output and for a white diffuse object at 1.3 meter. In this system, it is not possible to decrease the illuminating intensity because of the relatively low sensitivity of the crystal.

Systems with frontal objective of 50 mm focal length opened at 1.2 can work with typically 400 mW of laser output, for the same object placed at 1 meter and the same area visualized, but the final interferograms have a lower modulation, due to the higher amount of diffuse light. Nevertheless it does not affect greatly the final phase image. In this last case, the average level of the interferograms is also lower, this problem can be solved by using more sensitive CCD cameras. In this last system (S2 and S3) special attention must be paid to optical quality and cleanliness of the optical conponents and crystal which are located at the level of an intermediate imaging plane. The final imaging stage of S3 is less good than the one of S2 at point point of view of light collection (its aperture is lower), but also for the diffuse light that is collected.

6. REFERENCES

1. Ed. P.K. Rastogi, *Holographic interferometry : Principles and Methods*, Springer Series in Optical Sciences, Vol 68, Springer-Verlag, Berlin, 1994.
2. Ed. P. Günter and J.-P. Huignard, *Photorefractive Materials and their applications : Survey of Applications*, Topics in Applied Physics, Vol 62, Springer-Verlag, Berlin, 1989.
3. M.P. Petrov, S.I. Stepanov and A.V. Khomenko, *Photorefractive crystals in Coherent Optical Systems*, Springer Series in Optical Sciences, Vol 59, Springer-Verlag, Berlin, 1991.
4. S.I. Stepanov, Rep. Prog. Phys., Vol. 57, N°1, pp. 39-116, 1994.
5. R.C. Troth and J.C. Dainty, Opt. Lett., **16 (1)**, p. 53-55 (1991)
6. D. Dirksen and G. Von Bally, J. Opt. Soc. Am. B, **11 (9)**, p. 1858-1863 (1994)
7. M.P. Georges, Ph.C. Lemaire, "Real time holographic interferometer with BSO crystal using phase-shifting for quantitative deformation measurements", Technical Digest of NIST/OSA Conference on Photorefractive Materials Effects and Devices, Estes Park, Colorado, USA, paper WA1., June 1995.
8 M.P. Georges, Ph.C. Lemaire, "Phase-shifting real time interferometry that uses bismuth silicon oxide crystals", Applied Optics, Vol. 34, N°32, pp. 7497-7506, November 95.
9. L. Labrunie, G. Pauliat, J.-C. Launay and G. Roosen, "Unambiguous determination of object displacement in double exposure interferometry with photorefractive materials", Proceeding of ESO-SFO Conference on Optics and Information, Mulhouse, France, paper 7.2, October 1995.
10. A.A. Kamshilin and M.P. Petrov, Opt. Comm., **53 (1)**, p. 23-26 (1985)
11. S. Mallick, D. Rouède and A.G. Apostolidis, J. Opt. Soc. Am. B, **4 (8)**, p.1247-1259 (1987)
12. A. Marrakchi, R.V. Johnson and A.R. Tanguay, Jr., J. Opt. Soc. Am. B, **3 (2)**, p.321-336 (1986)